Supplement of The Cryosphere, 17, 5131–5136, 2023
https://doi.org/10.5194/tc-17-5131-2023-supplement

The Cryosphere Open Access EGU

Supplement of

Brief communication: Surface energy balance differences over Greenland between ERA5 and ERA-Interim

Uta Krebs-Kanzow et al.

Correspondence to: Uta Krebs-Kanzow (uta.krebs-kanzow@awi.de)

The supplement material is a compilation of additional diagnostics. As the main article focuses on differences between ERA5 and ERAI during the summer months, we here also provide a similar comparison for the annual mean properties (Figures S2, S6). Additionally, we present the interannual variability of summer means and annual means (Figures S1 and S3) and motivate the choice of lapse rate correction below.

A Choosing the lapse rate for downscaling to high resolution

To constrain the downscaling lapse rate, we analyze multiannual seasonal means of 2m-temperatures for both reanalysis products and select for each grid point its eight neighboring grid points. Among these we identify that pair (I_{low}, I_{high}) with maximal height difference $\Delta h = h(I_{high}) - h(I_{low})$ and calculate the respective temperature difference $\Delta T = \mathrm{T2M}(I_{high}) - \mathrm{T2M}(I_{low})$. We then define the local slope lapse rate (SLR) for regions with a sufficient height difference of more than $10\,\mathrm{m}$ as

$$\mathrm{SLR} = \begin{cases} \frac{\Delta T}{\Delta h} & |\Delta h| > 10\,\mathrm{m} \\ \text{n.a.} & \text{otherwise} \end{cases} \tag{1}$$

Figure S4 shows local summer slope lapse rates diagnosed from multiannual seasonal means for both reanalysis products. Since ERA5 has a higher horizontal resolution, we detect a more fine-scale structure in the ERA5's SLR. Away from the ice sheet's margins, diagnosed slope lapse rates range from the dry adiabatic lapse rate $-10\,\mathrm{K\,km^{-1}}$ at high altitude to approximately $-5\,\mathrm{K\,km^{-1}}$ at lower altitudes. Towards the ice sheet margins, the structure in SLR becomes more complex which indicates that under the influence of the surrounding land or ocean other factors are dominantly controlling the temperature distribution. The obtained slope lapse rates generally agree with the analysis of Erokhina et al. (2017), which has detected slope lapses rates in the range between $-5.9\,\mathrm{K\,km^{-1}}$ and $-9.1\,\mathrm{K\,km^{-1}}$ annually and between $-4.3\,\mathrm{K\,km^{-1}}$ and $-7.9\,\mathrm{K\,km^{-1}}$ for the summer, respectively.

We apply different lapse rates to uncover if the found 2m-air temperature difference between ERA5 and ERAI can be in part explained by differences in the underlying orographic boundary conditions (Fig. S5 and S6). We apply lapse rates of $0\,\mathrm{K\,km^{-1}}$, $-5\,\mathrm{K\,km^{-1}}$, $-7\,\mathrm{K\,km^{-1}}$, and $-10\,\mathrm{K\,km^{-1}}$ to cover the entire value range. Consistent with the analysis of local slope rates, we find that temperature differences appear overall reduced for lapse rates of $-5\,\mathrm{K\,km^{-1}}$, $-7\,\mathrm{K\,km^{-1}}$in summer.

Finally, we find that applying a lapse rate of $-5\,\mathrm{K\,km^{-1}}$ improves the agreement between reanalysis and measured in situ near-surface temperatures from the PROMICE network (Fausto et al., 2021; Ahlstrøm et al., 2008) with respect to the root mean square error of the monthly data (Fig. S7). We thus consider a lapse rate of $-5\,\mathrm{K\,km^{-1}}$ suitable to downscale summer temperatures to the higher resolution.

References

Ahlstrøm, A. P., Gravesen, P., Andersen, S. B., van As, D., Citterio, M., Fausto, R. S., Nielsen, S., Jepsen, H. F., Kristensen, S. S., Christensen, E. L., Stenseng, L., Forsberg, R., Hanson, S., Petersen, D., and Team, P. P.: A new programme for monitoring the mass loss of the Greenland ice sheet, Geological Survey of Denmark and Greenland Bulletin, pp. 61–64, 2008, http://www.geus.dk/DK/publications/geol-survey-dk-gl-bull/15/Documents/nr15%7B%5C_%7Dp61-64.pdf.

Erokhina, O., Rogozhina, I., Prange, M., Bakker, P., Bernales, J., Paul, A., and Schulz, M.: Dependence of slope lapse rate over the Greenland ice sheet on background climate, Journal of Glaciology, 63, 568–572, https://doi.org/10.1017/jog.2017.10, 2017.

Fausto, R., As, D., Mankoff, K., Vandecrux, B., Citterio, M., Ahlstrøm, A., Andersen, S., Colgan, W., Karlsson, N., Kjeldsen, K., Korsgaard, N., Larsen, S., Nielsen, S., Pedersen, A., Shields, C., Solgaard, A. & Box, J. Programme for Monitoring of the Greenland Ice Sheet (PROMICE) automatic weather station data. *Earth System Science Data*. **13**, 3819-3845 (2021), https://dx.doi.org/10.5194/essd-13-3819-2021.

Figures

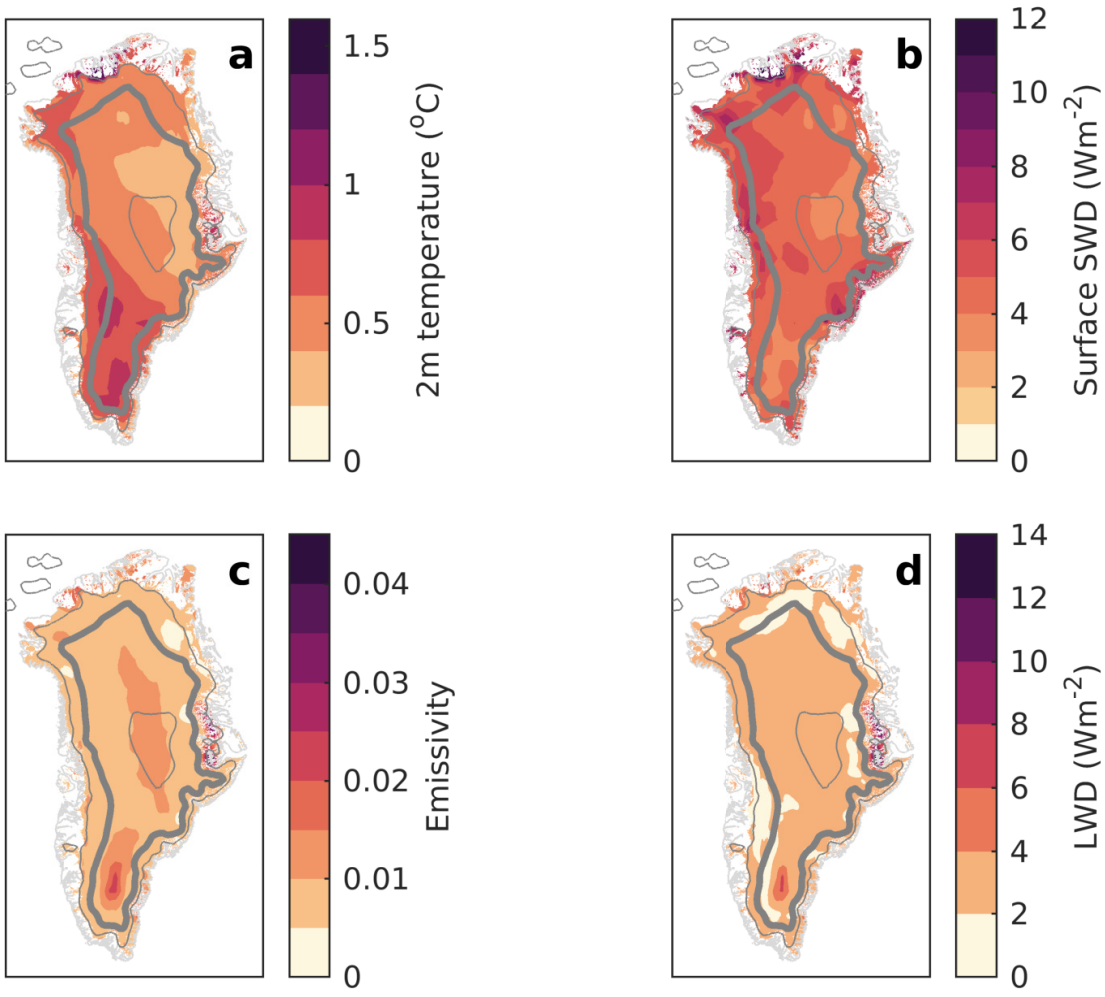

Figure S1. Standard deviation of differences between ERA5 and ERAI in summer means for the period 1979–2018: 2m-air temperature (top left), downward shortwave radiation (top right), emissivity (bottom left), and cloud over (bottom right). The annual fields are shown in Figure S3. The countour lines indicates an elevation of 1000 m, 2000 m, and 3000 m.

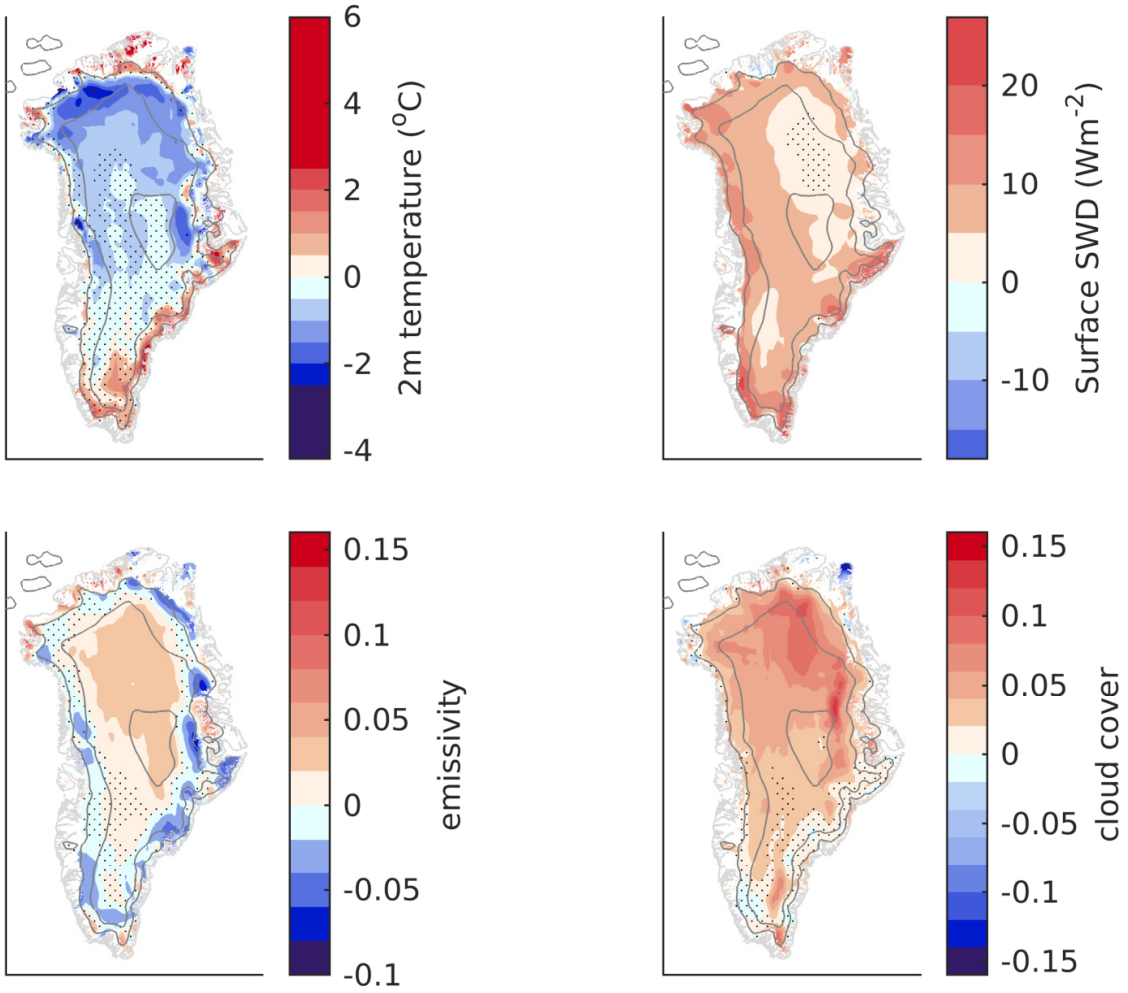

Figure S2. Multiyear annual mean difference between ERA5 and ERAI for the 1979–2018 period in 2m-air temperature (upper left), downward shortwave radiation (upper right), emissivity (lower left), and cloud cover (lower right), stippling indicates regions where the mean difference is smaller than two standard deviations of its interannual variability. The contour line follows the elevation of 1000 m, 2000 m, and 3000 m.

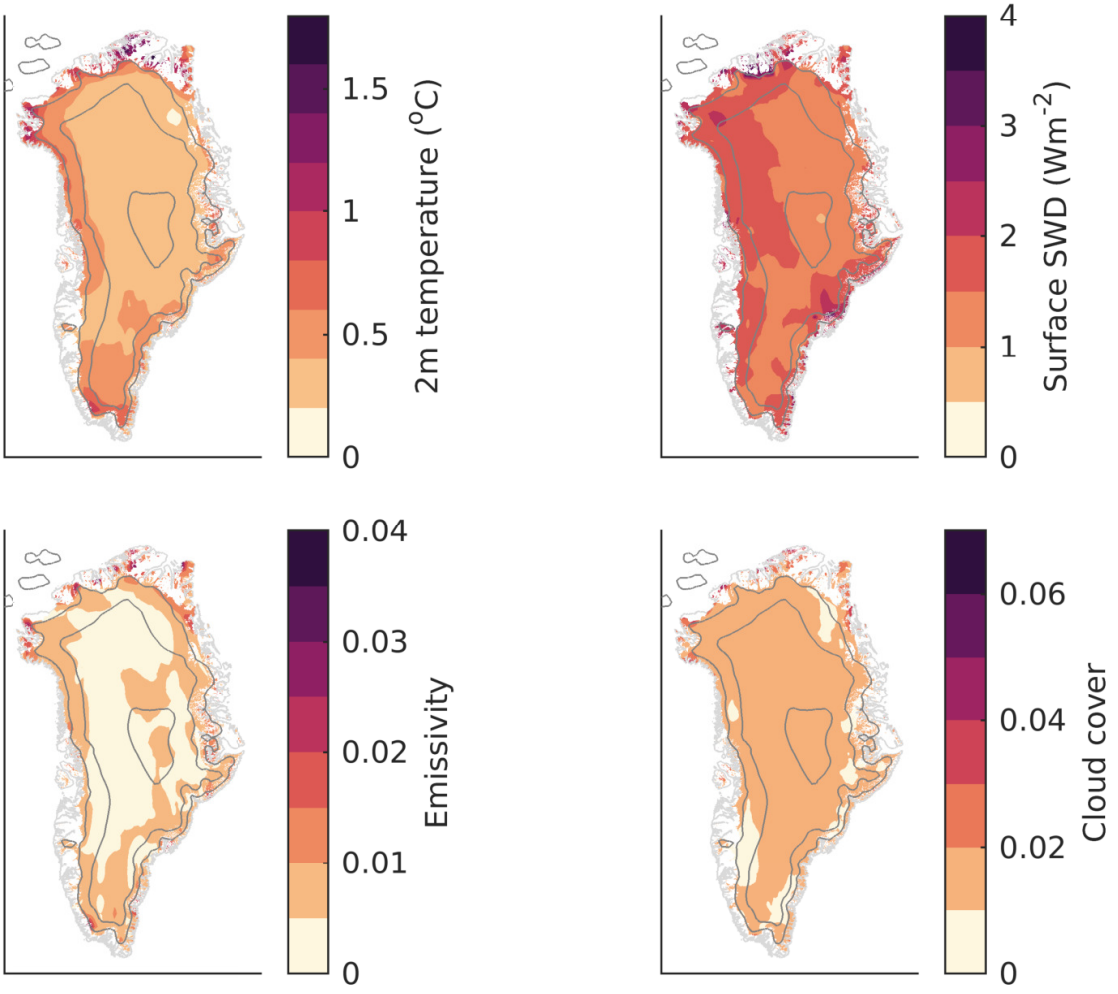

Figure S3. Same as Figure S1 but for annual means.

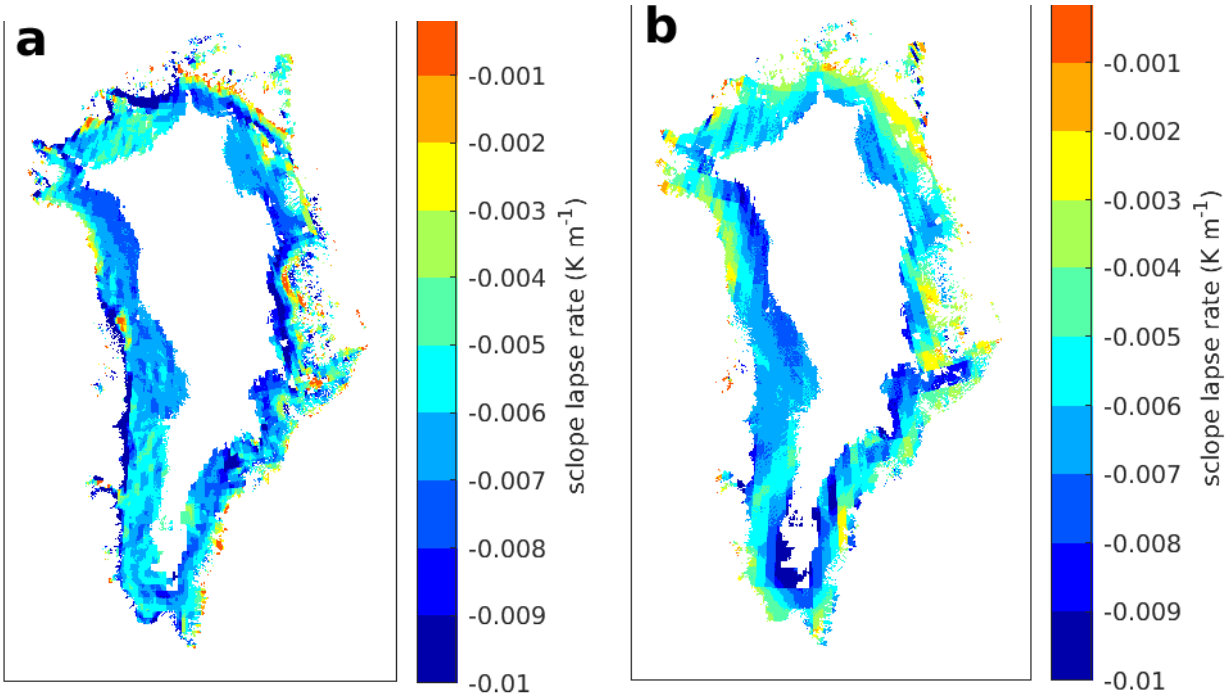

Figure S4. Slope lapse rates as diagnosed from ERA5 (a) and ERAI (b) for summer mean 2m-air temperature in the period 1979–2018.

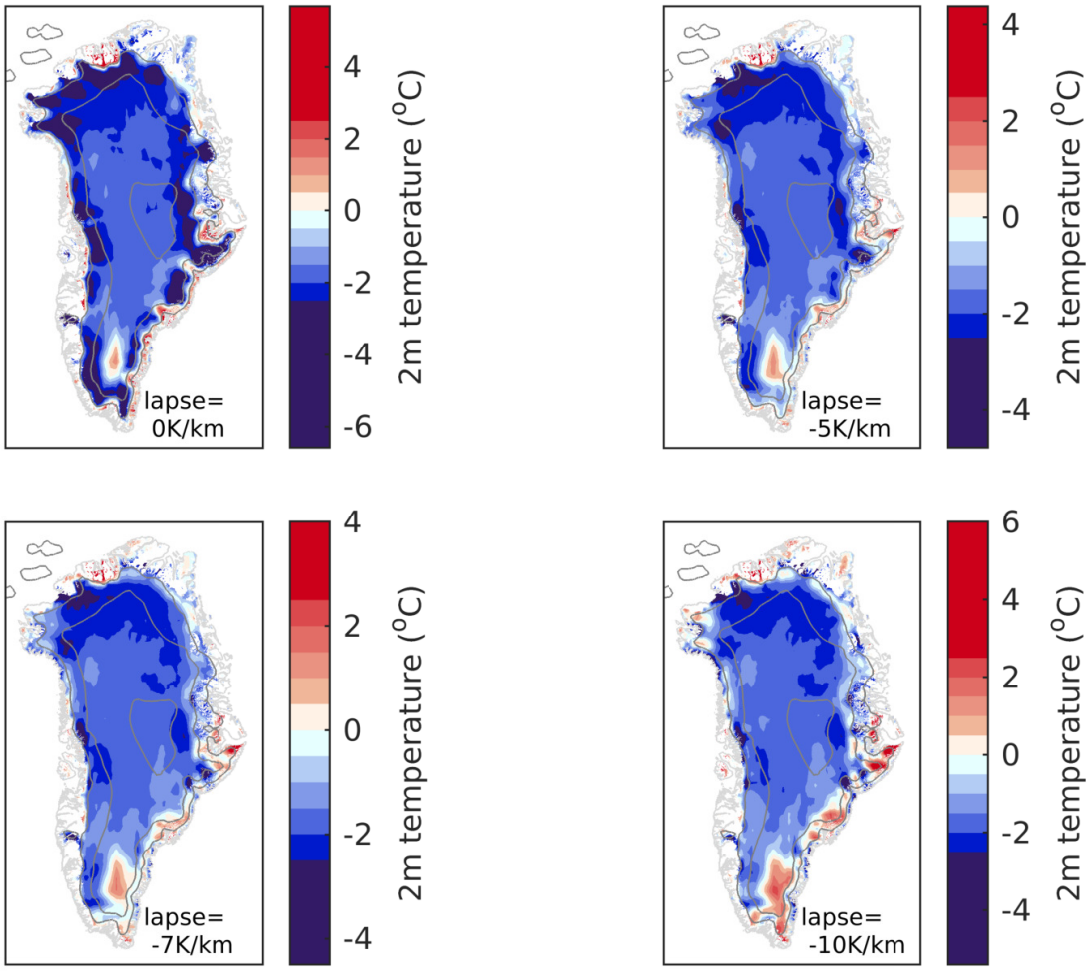

Figure S5. Mean difference of summer means of the 2m-air temperature between ERA5 and ERAI over the GrIS in the 1979–2018 period without lapse rate corrections (top left), and lapse rate correction of $-5\,\mathrm{K\,km^{-1}}$ (top right), $-7\,\mathrm{K\,km^{-1}}$ (bottom left) and $-10\,\mathrm{K\,km^{-1}}$ (bottom right). Contour lines illustrate $1000\,\mathrm{m}$, $2000\,\mathrm{m}$, and $3000\,\mathrm{m}$ elevation. Please note the different color scales for each subplot.

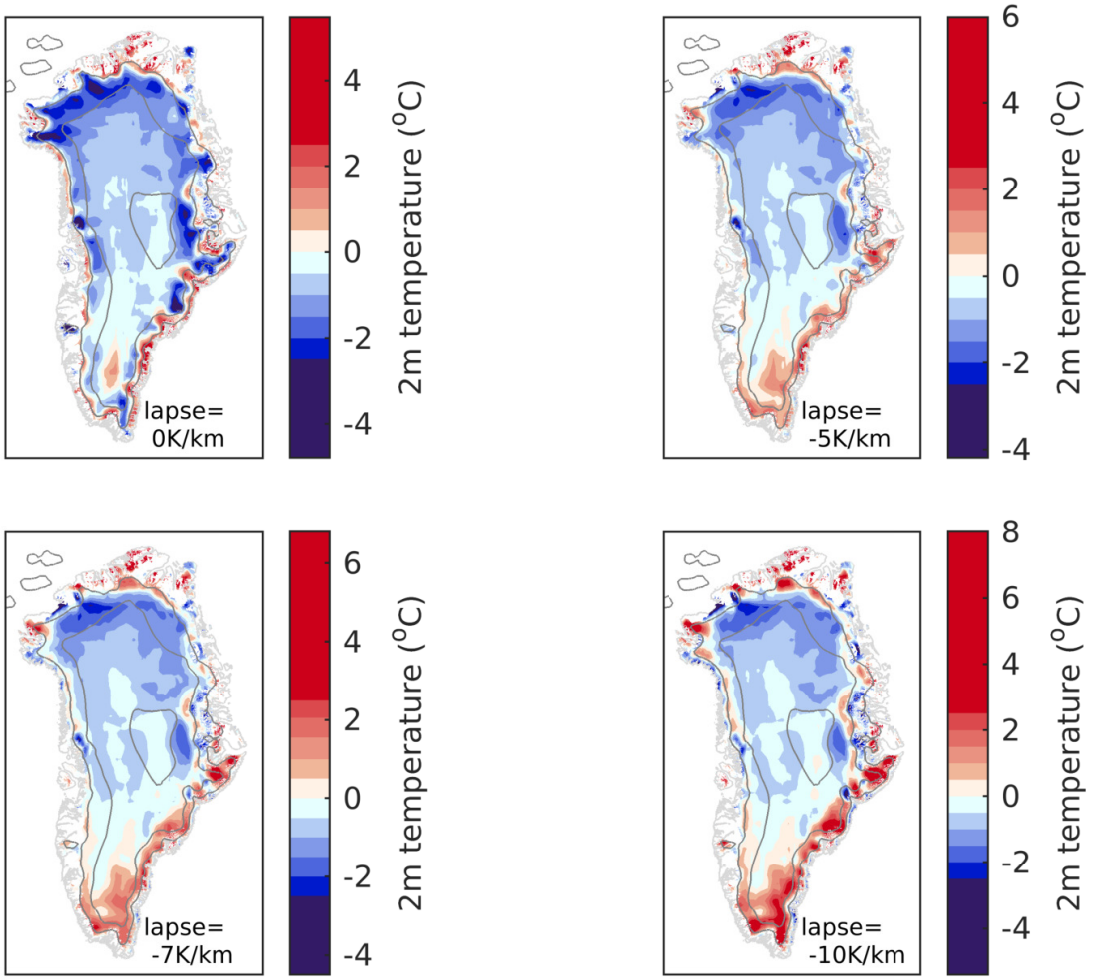

Figure S6. Same as Figure S5 but for mean difference of annual means.

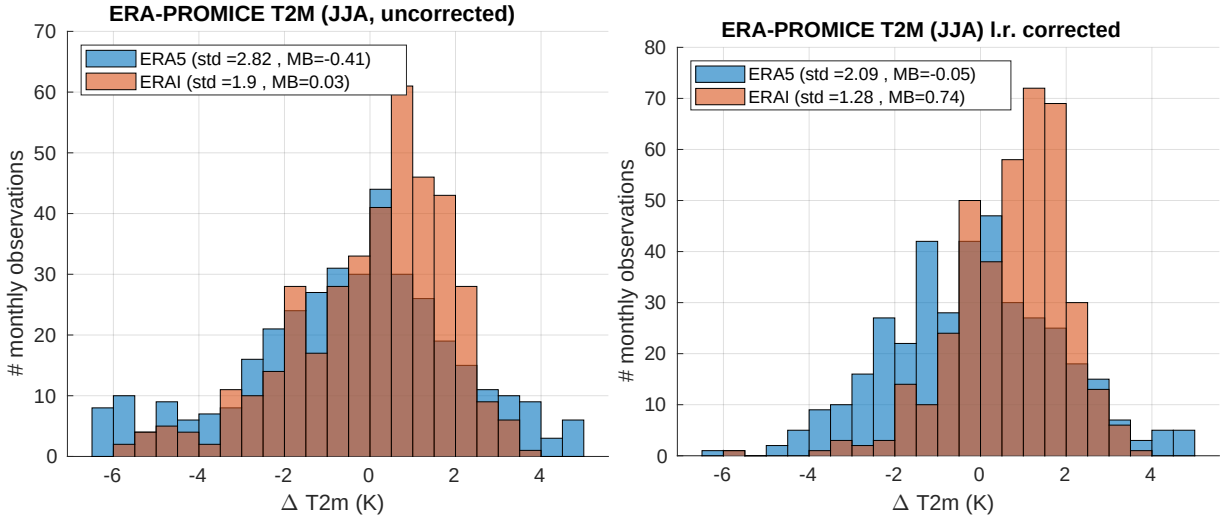

Figure S7. Distribution of ERA5 and ERAI bias to monthly PROMICE observations for the 2007–2016 summer months (i.e., June, July, and August, JJA) for 2m-air temperatures without applying a lapse rate correction (left) and with a lapse rate correction of $-5\,\mathrm{K\,km}$ (right). The text box insets provide standard deviation (std) and mean biases (MB) for the respective distributions.

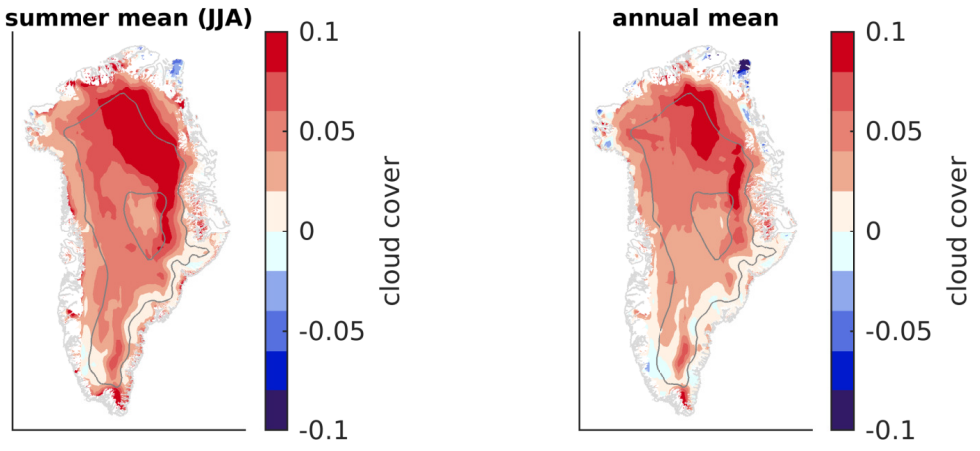

Figure S8. Multiyear summer mean (left) and annual mean (right) differences between ERA5 and ERAI cloud cover for the 1979–2018 period

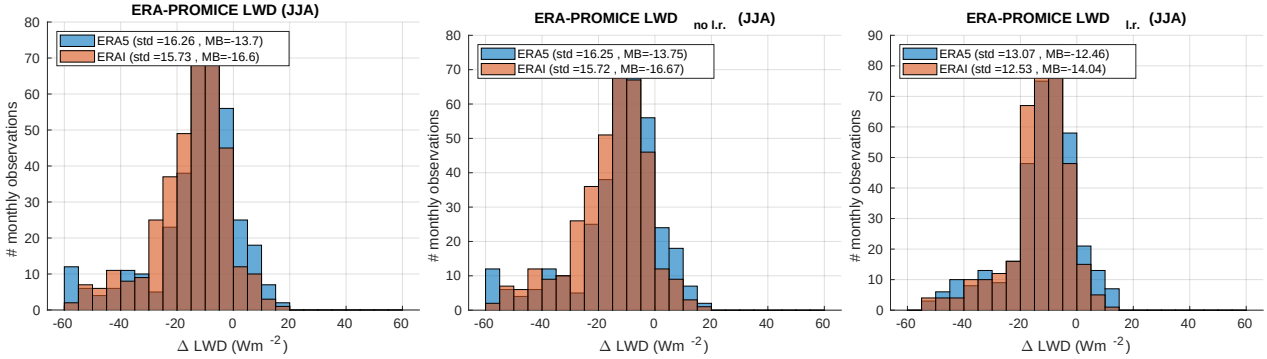

Figure S9. Distribution of ERA5 and ERAI bias to monthly PROMICE observations for the 2007–2016 summer months (i.e., June, July, and August, JJA) for LWD (left), for LWD recalculated from emissivity and uncorrected T2m (center) and for LWD recalculated from emissivity and lapse rate corrected T2m (right). The text box insets provide standard deviation (std) and mean biases (MB) for the respective distributions.

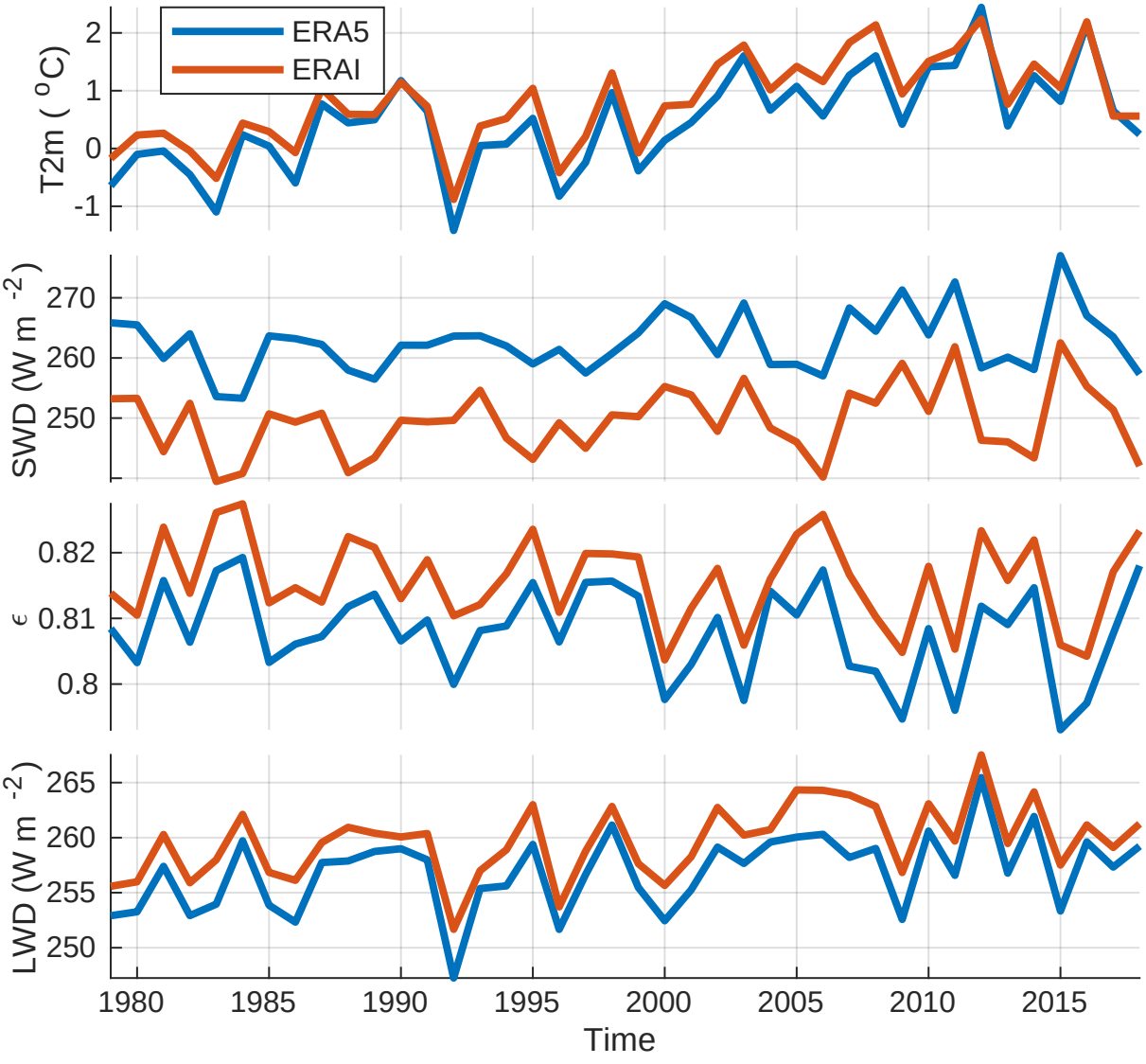

Figure S10. 1979–2016 yearly summer means of interpolated (a) lapse rate corrected 2m-air temperature, (b) downward surface shortwave radiation, (c) emissivity, and (d) downward longwave radiation for ERA5 (blue) and ERAI (red) averaged over the 0 m to 1000 m elevation range of the GrIS.

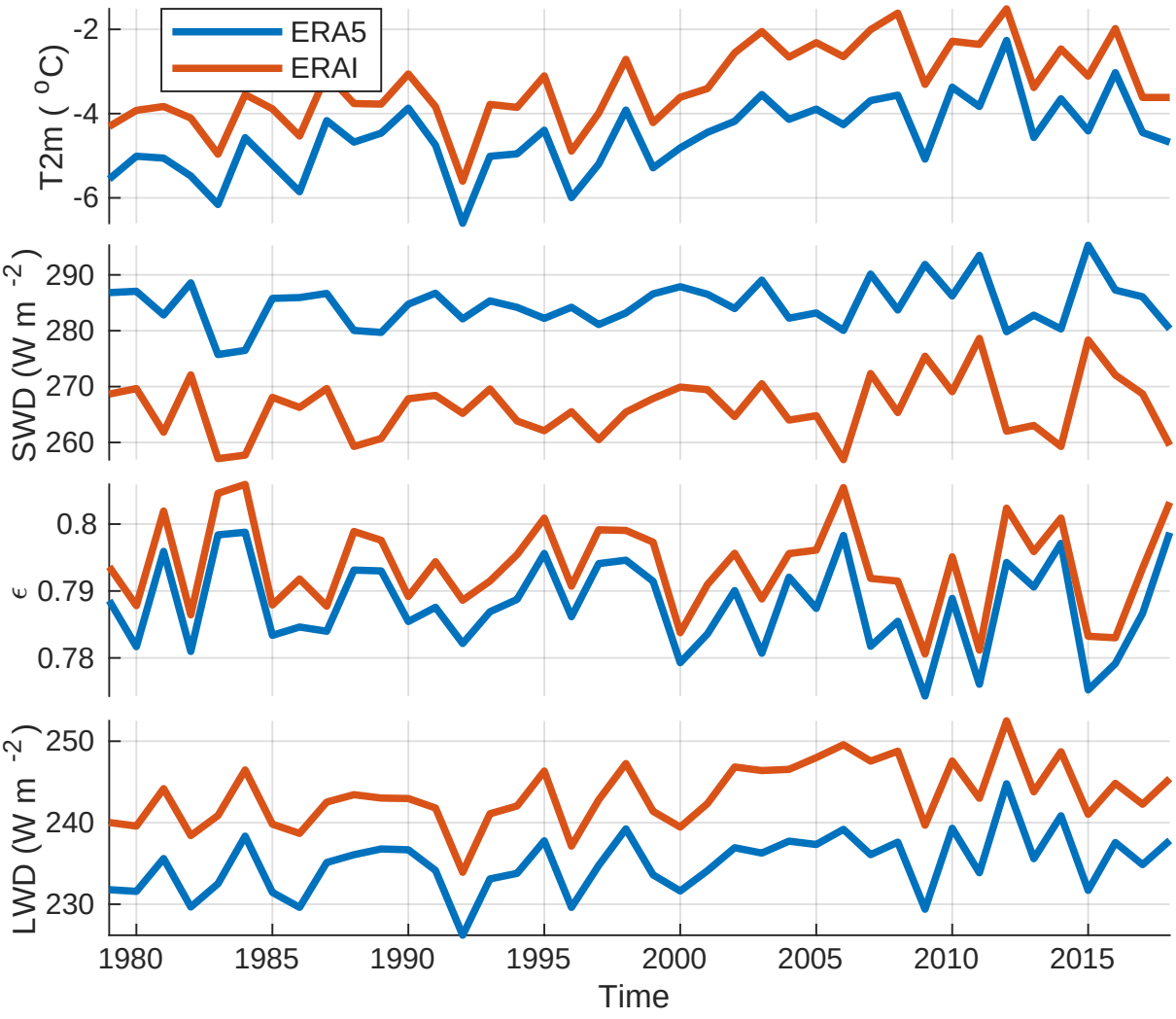

Figure S11. 1979–2016 yearly summer means of interpolated (a) lapse rate corrected 2m-air temperature, (b) downward surface shortwave radiation, (c) emissivity, and (d) downward longwave radiation for ERA5 (blue) and ERAI (red) averaged over the 1000 m to 2000 m elevation range of the GrIS.

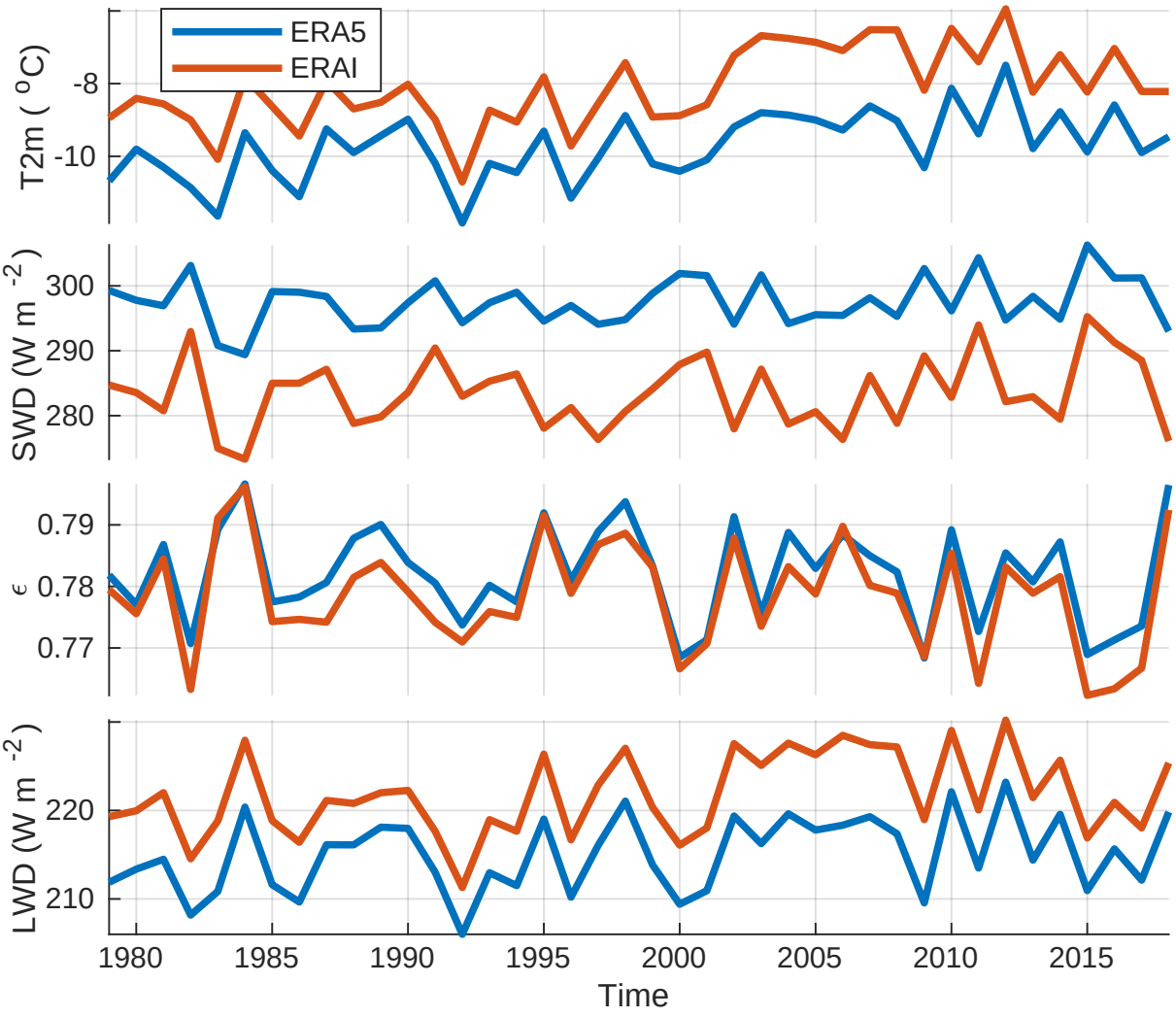

Figure S12. 1979–2016 yearly summer means of interpolated (a) lapse rate corrected 2m-air temperature, (b) downward surface shortwave radiation, (c) emissivity, and (d) downward longwave radiation for ERA5 (blue) and ERAI (red) averaged over the 2000 m to 3000 m elevation range of the GrIS.

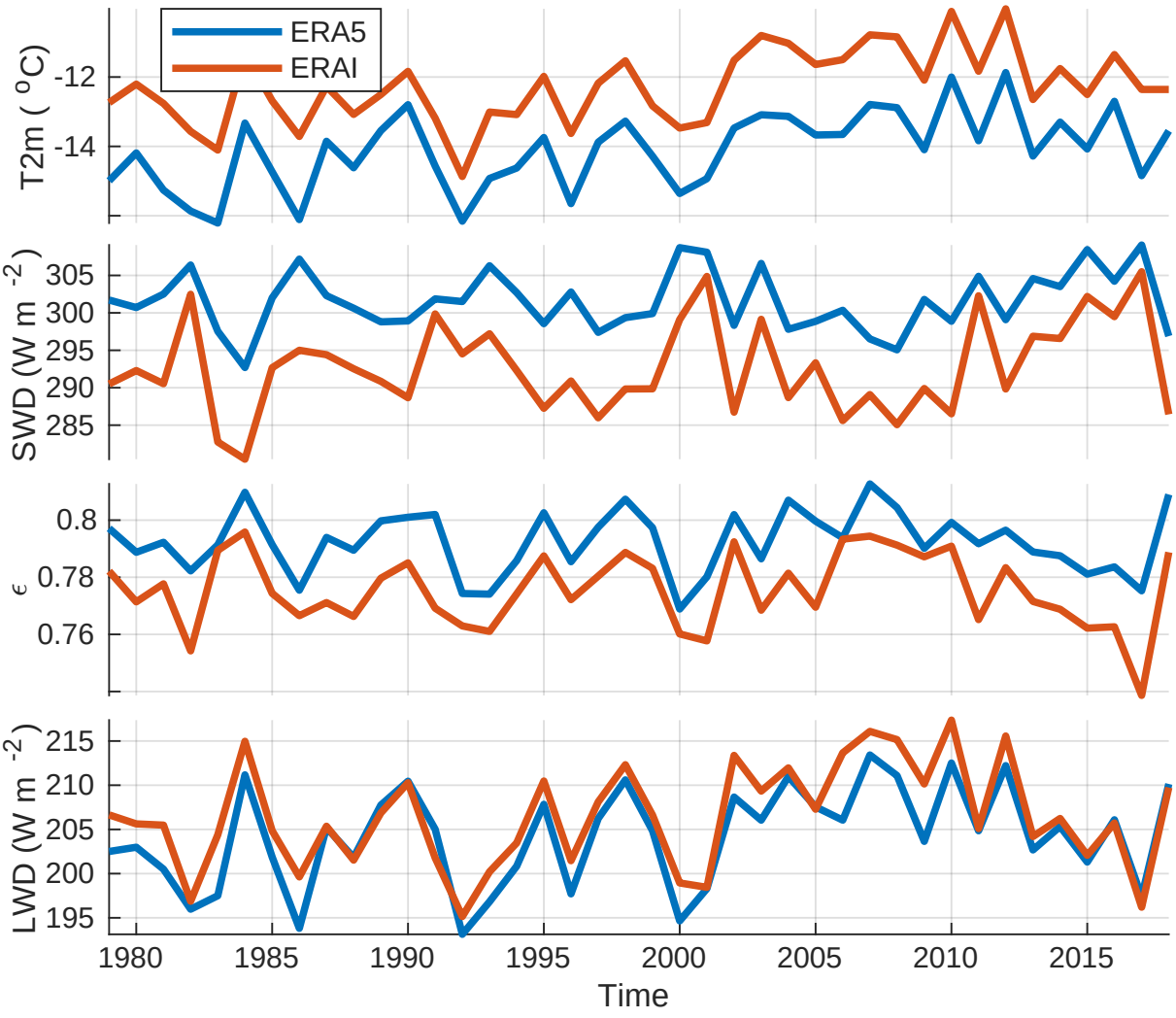

Figure S13. 1979–2016 yearly summer means of interpolated (a) lapse rate corrected 2m-air temperature, (b) downward surface shortwave radiation, (c) emissivity, and (d) downward longwave radiation for ERA5 (blue) and ERAI (red) averaged over the 3000 m to 4000 m elevation range of the GrIS.